THE RIGIDITY OF A PARTIALLY TRIANGULATED TORUS

J. CRUICKSHANK, D. KITSON AND S.C. POWER

ABSTRACT. A simple graph is 3-rigid if its generic embeddings in $\mathbb{R}^3$ are infinitesimally rigid. Necessary and sufficient conditions are obtained for the minimal 3-rigidity of a simple graph obtained from a triangulated torus by the deletion of edges interior to an embedded triangulated disc.

1. INTRODUCTION

The graph $G = (V, E)$ of a triangulated sphere is generically 3-rigid in the sense that any generic placement of the vertices in three-dimensional Euclidean space determines a bar-joint framework which is continuously rigid. This generic version of Cauchy's rigidity theorem for convex polyhedra follows from Dehn's determination [4] of the infinitesimal rigidity of convex triangulated polyhedra. See also Gluck [7] for an alternative proof. Moreover, the graphs of triangulated spheres are minimally 3-rigid since Maxwell's necessary condition $|E| \geq 3|V| - 6$ holds with equality. Although this fact is prominent in combinatorial rigidity little seems to be known about the minimal rigidity of general triangulated surfaces and manifolds.

We note that Fogelsanger [5] has shown that a finite simple graph given by a triangulated compact surface without boundary is 3-rigid. The proof is an extended argument employing combinatorial edge contraction methods to reduce to the case of a complete graph, which is evidently 3-rigid. The methods also extend to higher dimensions. However, with the exception of the sphere the triangulated surface graphs without boundary are over-constrained, in the sense that $|E| > 3|V| - 6$.

In what follows we begin a systematic analysis of minimal 3-rigidity for the graphs of triangulations of surfaces with boundaries by considering certain partially triangulated tori that satisfy equality in the Maxwell condition. Our main result is a necessary and sufficient condition for minimal 3-rigidity in the case of a partially triangulated torus graph which has edges removed from the interior of an embedded triangulated disc. A precise definition of these graphs, together with their inherited facial structure and integral homology, is given in Section 2. Moreover we show that (i) there are 17 distinct forms of boundary graph for this class, (ii) there are 2 irreducible graphs, and (iii) the graphs are generated from these two irreducibles by vertex splitting.

There is currently considerable interest in determining conditions for the rigidity of nongeneric bar-joint frameworks, and particularly those with prescribed symmetry groups. See, for example, Connelly et al [2] and Schulze and Tanigawa [9] where symmetric variants

of Maxwell counting conditions play a key role. We shall be concerned entirely with generic frameworks but the results and methods may nevertheless give insights into the rigidity of symmetric toroidal structures.

The main theorem may be stated as follows.

Theorem 1.1. *Let G be a torus with hole graph. Then the following conditions are equivalent.*

    (i) G is minimally 3-rigid.
   (ii) G is $(3,6)$-tight.
  (iii) G is constructible from K_3 by vertex splitting.

While $(3,6)$-tightness is a well-known necessary condition (see Section 3 for the definition) its sufficiency here is a more subtle issue than in the case of the generic Cauchy theorem. For example, we note in Section 3 that the substitution of a triangulated subdisc by a triangulated disc with the same boundary need not preserve $(3,6)$-tightness. Also we see that there are torus graphs with two holes which are $(3,6)$-tight and yet are generically flexible.

The development is structured as follows. In Section 2 a *torus with hole graph* is formally defined. In Section 3 we consider the subfamily $\mathcal{T}$ of $(3,6)$-tight graphs G of this type and we give the 17 possible forms for the boundary graphs. In Section 4 we define *critical separating cycles* and associated *fission moves* within the class $\mathcal{T}$. Exploiting the toroidal facial structure of the graphs in $\mathcal{T}$ we obtain a key lemma, Lemma 4.4, which shows that if the contraction of an edge e preserves the simplicity of the graph but violates the $(3,6)$-tight sparsity count then there exists a critical separating cycle through e. In this case an associated fission move $G \to \{G_1, G_2\}$ is possible, which provides a pair of strictly smaller graphs in $\mathcal{T}$ if $|V(G)| \geq 10$. It follows that there is a contraction-fission reduction scheme to a certain family of small graphs in $\mathcal{T}$ with no more than 9 vertices.

In Section 5 we prove that the graphs in $\mathcal{T}$ with no more than 8 vertices are 3-rigid and that the 9 vertex graphs in $\mathcal{T}$ are contractible in $\mathcal{T}$. The inverse move for edge contraction is a vertex splitting move, which is known to preserve 3-rigidity (Whiteley [10]). Also the inverse fission moves, or fusion moves, are rigid subgraph substitution moves preserving 3-rigidity, and so the equivalence of (i) and (ii) follows. We note that critical separating cycle methods have also proven useful recently in a simpler reduction scheme for modified triangulated spheres (Cruickshank, Kitson and Power [3]) and we expect this methodology to be a key tool in the analysis of higher genus surface graphs.

In Section 6 we give an alternative proof of the equivalence of (i) and (ii) which is more direct. The proof is based on (a), a nested application of the key lemma, in order to identify a contractible edge whose contraction preserves membership in $\mathcal{T}$, and (b) an analysis of the graphs of $\mathcal{T}$ which are not contractible in this manner. This leads to the fact that there are 2 such irreducible graphs (see Theorem 6.2). Each of these irreducible graphs is constructible from K_3 by vertex splitting and so the equivalence of (i), (ii) and (iii) follows.

2. Surface graphs in the torus

Let $\mathcal{M}$ be a classical compact surface of finite genus, with or without a boundary. In this case we may define a *surface graph for* $\mathcal{M}$ to be the graph determined by the 1-skeleton of a simplicial complex with geometric realisation $\mathcal{M}$, when this 1-skeleton graph is simple. Equivalently $\mathcal{M}$ is the graph determined by a *triangulation* of $\mathcal{M}$ in the usual sense, which requires simplicity [8]. However, the 1-skeleton perspective is the most useful for us since we are interested in graphs associated with modified compact surfaces which have superficial holes, obtained by the removal of embedded open discs. These spaces, as is evident in the figures below for example, are more general than classical surfaces with boundaries.

We refer to a surface graph for the torus as a *torus graph* while a surface graph for the disc is referred to as a *triangulated disc*.

Definition 2.1. Let M be a simplicial complex for the torus whose 1-skeleton is a simple graph T. Let D be the simplicial complex of a triangulated disc and let ι be an injective map from the set of 2-simplexes of D to the set of 2-simplexes of M which respects the adjacency relation between 2-simplexes of D. Finally, let G be the subgraph of T obtained by deleting the edges associated with the 1-simplexes which are images, under the map induced by ι, of the interior 1-simplexes of D. Then G is said to be a *torus with hole graph*.

We also view a torus with hole graph G as being endowed with the *facial structure* inherited from M. This consists of the set of 3-cycles for the faces that are not in the range of ι. Thus G has well-defined simplicial integral homology groups.

A torus with hole graph G is determined by a triple (M, D, ι) where $\iota : D \to M$ is a simplicial map from a simplicial complex D of a triangulated disc to a simplicial complex M, of the torus, which is injective on 2-simplexes. It is also convenient to abuse notation and let D, T and ∂D denote the graphs of the simplicial complexes D, M and ∂D. Also we write i for the associated simple graph homomorphism $i : D \to T$. We refer to a subgraph of G as an *embedded triangulated disc graph* if it has the form $j(H)$, where H a triangulated disc and $j : H \to T$ is graph homomorphism which is injective on facial 3-cycles.

The *boundary graph* ∂G of a torus with hole graph G is the subgraph whose edges do not lie in two facial 3-cycles of G. Thus ∂G is the graph $i(\partial D)$.

A torus with hole graph G is also endowed with a closed path of edges that cover the edges of ∂G, perhaps with repetition. This path is the image under ι of the boundary cycle of the graph D. We also refer to the graph homomorphism

$$\alpha = i|_{\partial D} : \partial D \to \partial G,$$

as the *detachment map* of G. This map has the form $\alpha : C_r \to \partial G$ where C_r is the r-cycle graph, and is uniquely associated with G.

We now note some examples of torus with hole graphs.

Let $\mathcal{M}$ be the compact surface with boundary derived from $S^1 \times S^1$ by the removal of the interior of a closed topological disc $\mathcal{D}$, where the topological boundary $\partial \mathcal{D}$ is a *simple* closed curve. Then a surface graph for $\mathcal{M}$ is a torus with hole graph. These graphs correspond to the injectivity of the detachment map. Figure 1 illustrates such a graph.
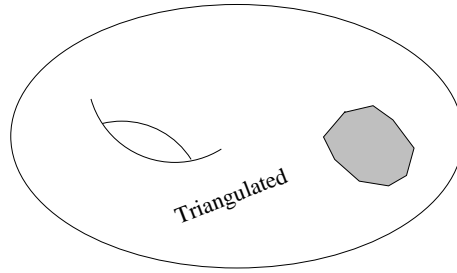
FIGURE 1. A torus with hole graph (with shaded superficial hole).

On the other hand Figure 2 indicates a torus with hole graph for which α is not injective and for which

$$|V(\partial G)| = |V(\partial D)| - 1, \quad |E(\partial G)| = |E(\partial D)|$$
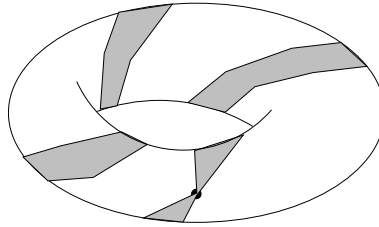

FIGURE 2. A torus with hole graph with noninjective detachment map.

Recall that a simple graph G is 3-connected if there exists no pair of vertices x, y which separates the graph in the sense that there are vertices v, w such that each path from v to w contains one of the vertices in the pair. We note that a torus with hole graph may fail to be 3-connected, as indicated in Figure 3. However, we shall see that the combinatorial condition of $(3, 6)$-tightness, defined in the next section, limits the possible forms of noninjectivity of the detachment map. In particular these graphs are necessarily 3-connected.
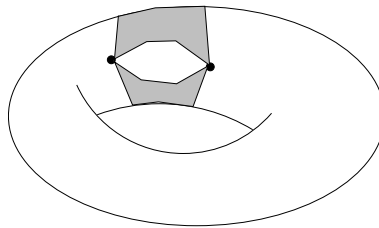

FIGURE 3. A torus with hole graph which is not 3-connected.

Figure 4 gives a perspective view of two torus with hole graphs with noninjective detachment map which can arise as $(3,6)$-tight graphs. Here we may regard the detached disc interior (the hole) as being wrapped around the torus. The graph of the second figure has an exposed edge, that is, one which is incident to no face. This arises when the detachment map α is noninjective on edges.
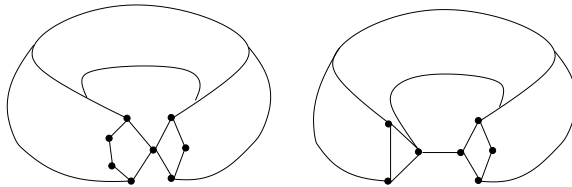

FIGURE 4. Perspective figures of torus with hole graphs.

Finally, we remark that a torus with hole graph G may take an extreme form with $\partial G = G$. In particular G may consist of two cycles of edges joined at a single vertex. Evidently such graphs are not $(3,6)$-tight.

2.1. **Planar representations.** We find it convenient to illustrate torus with hole graphs by *rectangular face graph* representations. A rectangular face graph for a torus graph may be formally defined as a planar triangulated disc R whose outer boundary path ∂R, as a directed cycle of edges, is a concatenation $\partial R = \pi_1\pi_2\pi_3\pi_4$ where π_1 and π_3 are paths of length r, π_2 and π_4 are paths of length s, and where these paths are appropriately identified. This identification corresponds to bijections $V(\pi_1) \to V(\pi_3)$ and $V(\pi_2) \to V(\pi_4)$ which are order reversing. The associated identification graph $R/\sim$ is a torus graph. If D is a triangulated disc in R and R' is obtained from R by the removal of edges interior to D, then the identification graph $G = R'/\sim$ is a torus with hole graph.

The class of graphs in $\mathcal{T}$ with no more than 9 vertices is surprisingly rich and in the Appendix we use face graph representations extensively for their case-by-case analysis.

Additionally, it is useful to consider torus with hole graphs as embedded graphs on the topological torus, and we do this in the proofs of Lemmas 4.5, 5.3 and 5.7 for example. Thus a torus graph has an embedded graph representation in $[0,1]^2/\sim$ and the hole for a torus with hole graph can be viewed as an embedded open disc in the open subset $(0,1)^2$.

3. $(3,6)$-TIGHT TORUS WITH HOLE GRAPHS.

We now consider torus with hole graphs G which are $(3,6)$-tight and we give the 17 possible forms for a detachment map $\alpha : C_9 \to \partial G$.

Recall that the *freedom number* for a finite simple undirected graph $G = (V,E)$ is $f(G) = 3|V| - |E|$ and that if $f(G) = 6$ then G is said to satisfy the *Maxwell count*.

Lemma 3.1. *Let G be a torus with hole graph determined by the triple (T, D, i). Then G satisfies the Maxwell count if and only if ∂D is a 9-cycle.*

Proof. From Euler's formula it follows that $f(T) = 0$ if T is a surface graph for the torus. If ∂D has length r then G can be completed to a torus graph by the addition of $r - 3$ edges, and so $f(G) = 6$ if and only if $r = 9$.

$\qquad \square$

A simple graph G is $(3, 6)$-*tight* if $f(G) = 6$ and $f(K) \geq 6$ for every subgraph K with at least 3 vertices. We write $\mathcal{T}$ for the class of torus with hole graphs which are $(3, 6)$-tight.

Figure 5 indicates a rectangular face graph representation for a graph H_1 in $\mathcal{T}$ for which the boundary graph is a 9-cycle.
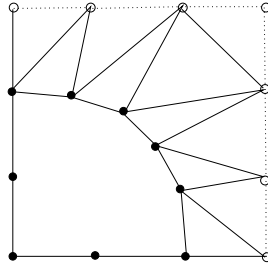

FIGURE 5. A rectangular face graph for the graph H_1.

It is elementary to verify that H_1 is $(3, 6)$-tight by means of the following principle. If a graph H_a arises from a $(3, 6)$-tight graph H_b by vertex splitting, in the sense of the following definition, then H_a is also $(3, 6)$-tight. In this way it also readily follows that the graphs $H_2, \ldots, H_{17}$ given below are graphs in $\mathcal{T}$.

Note that if H_1' is obtained from H_1 by retriangulation then H_1' need not be $(3, 6)$-tight. This is the case, for example, if H_1' has a path of edges around the hole which has length less that 9. In this case the path defines a torus with hole graph with freedom number less than 6. In general, replacing a triangulated disc by another with the same boundary need not preserve the $(3, 6)$-tightness of torus with hole graphs.

Let $G = (V, E)$ be a simple graph with vertices $v_1, v_2, \ldots, v_r$ and let $v_1 v_2, v_1 v_3, \ldots, v_1 v_n$ be the edges of E that are incident to v_1. Let $G' = (V', E')$ arise from G by the introduction of a new vertex v_0, new edges $v_0 v_1, v_0 v_2, v_0 v_3$, and the replacement of any number of the remaining edges $v_1 v_t$, for $t > 3$, by the edges $v_0 v_t$. Then the move $G \to G'$ is said to be a *vertex splitting* move on v_1.

The proof of rigidity preservation under vertex splitting is due to Whiteley [10]. A different proof, together with a proof of Gluck's theorem, is given in Cruickshank, Kitson and Power [3].

3.1. **Graphs in $\mathcal{T}$ with noninjective detachment map.** When the detachment map α is not injective the closed path $i(\partial D)$ can be regarded as a 9-cycle which has been pinched together in some manner, with several self-contact points. The simplest form of this occurs when $|V(\partial G)| = 8$ and we note that ∂G then takes one of two forms, which we denote as $v3v6$ and $v4v5$. Figure 6 indicates the graphs H_2 and H_3 which are of these types.

In general a detachment map $\alpha : C_9 \to \partial G$ determines a vertex word of length 9 whose letters are the vertices of ∂G, with repetitions, ordered in correspondence with the 9-cycle of C_9. This word is uniquely determined up to cyclic permutation and order reversal. However, we shall employ the economy of writing the short form $v3v6$ for the full form $v_1 v_2 v_3 v_1 v_4 v_5 v_6 v_7 v_8$ where $v = v_1$ is a repeated vertex. The short form should be read as "v followed by 3 distinct edges to v, followed by 6 further distinct edges" (terminating in the first vertex v). An example of a cyclic word for a detachment map with 2 repeated vertices (and no repeated edges) is $v1w2v2w4$. The numbers represent the 9 distinct edges in $i(\partial D)$ in this example. We use the letters v, w and also x to denote repeated vertices. When edges are repeated we adopt a more economical notation. For example $e3e4$ indicates that edge e is repeated and that e is followed by 3 distinct edges then followed by e (even though traversed in a different order) which is then followed by 4 distinct edges to complete the cycle. We use the letters e, f, and g to denote repeated edges. In every cyclic word for the detachment map type the number of edge letters (e, f or g), counted with multiplicities, together with the total of the numerals, is equal to 9.
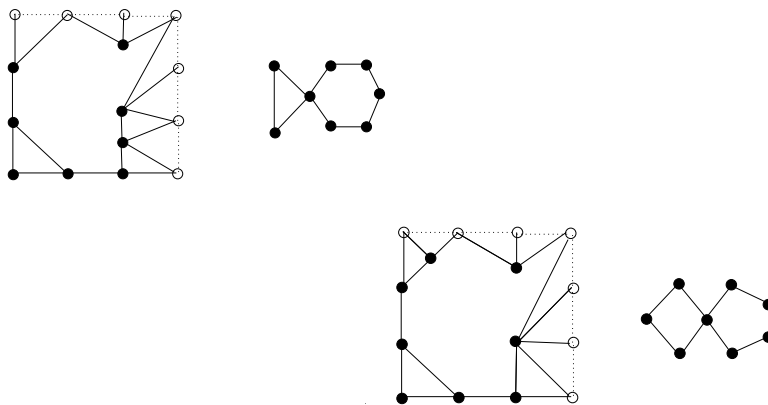

FIGURE 6. Rectangular face graph representatives for the graphs H_2 and H_3 in $\mathcal{T}$ with boundary graphs of type $v3v6$ and $v4v5$.

The next lemma and the table in Figure 7 show that even the small graphs in $\mathcal{T}$, with 9 or fewer vertices, form a surprisingly varied class. The proof of the lemma is a straightforward case-by-case analysis and is given in the Appendix.

Lemma 3.2. *There is a collection of graphs $H_1, \ldots, H_{17}$ in $\mathcal{T}$ with detachment maps $\alpha_i, 1 \leq i \leq 17$, and the following properties.*

(i) If $G \in \mathcal{T}$ with detachment map α then there is a unique graph H_i and a graph isomorphism $\phi : \partial H_i \to \partial G$ such that $\alpha = \phi \circ \alpha_i$.

(ii) $V(H_i) = V(\partial H_i)$, for each i.

We remark that the graphs H_{16} and H_{17} are uncontractible torus with hole graphs G in the sense that there are no edges belonging to two faces in G whose contraction yields a simple graph (and hence a torus with hole graph). On the other hand $H_1, \ldots, H_{15}$ do have such edges, referred to as FF edges in the next section.

Cyclic word	$G \in \mathcal{T}$
$v9$	H_1
$v3v6$	H_2
$v4v5$	H_3
$e3e4$	H_4
$v1w2v2w4$	H_5
$v1w2v3w3$	H_6
$v1w2v4w2$	H_7
$v1w3v2w3$	H_8
$v2w3v2w2$	H_9
$v1w2x1v2w1x2$	H_{10}
$v1w1x1v2w2x2$	H_{11}
$v3e2v1e1$	H_{12}
$v3e1v2e1$	H_{13}
$v2e2v2e1$	H_{14}
$v1e1w2v1e1w1$	H_{15}
$e1f2e1f1$	H_{16}
$ef1ge1fg1$	H_{17}

FIGURE 7. The cyclic words that label the 17 forms of detachment maps for graphs in $\mathcal{T}$.

3.2. **Torus graphs with several holes.** There is an evident modification of Def. 2.1 which defines a torus graph with *several* (superficial) holes. We note the following two examples which are also $(3, 6)$-tight. Figure 8 shows a rectangular face graph R_1 for a torus graph G_1 with two holes. Two triples of edges (dashed) have been deleted from the interiors of two triangulated discs in R_1. The graph G_1 is $(3, 6)$-tight and has a separating pair of vertices v, w. In particular it is not 3-rigid.
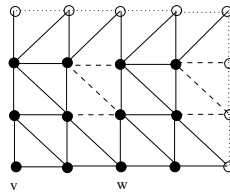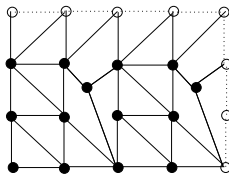

FIGURE 8. The rectangular face graph R_1

Figure 9 indicates a rectangular face graph R_2 for a torus graph G_2 with 6 holes. The graph G_2 may be obtained from G_1 by the addition of two degree 3 vertices and so G_2 is also $(3, 6)$-tight and fails to be 3-rigid.

FIGURE 9. The rectangular face graph R_2

4. CONTRACTION MOVES IN $\mathcal{T}$ AND CRITICAL SEPARATING CYCLES

Let G be a torus with hole graph. An edge of G is of *type FF* if it is contained in two facial 3-cycles and an FF edge is *contractible* if it is not contained in any non-facial 3-cycle. For such an edge there is a natural contraction move on the graph G which creates another torus with hole graph G'. To define this formally, let $e = vw$ be a contractible FF edge in G and let avw and bvw be the two facial 3-cycles which contain e. A simple graph G' is said to be obtained from G by an *edge contraction* on $e = vw$ if G' is obtained by (i) deleting the edges aw and bw, (ii) replacing all remaining edges of the form xw with xv, (iii) deleting the edge e and the vertex w. Note that G' is again a torus with hole graph with the natural facial structure inherited from G. Also G can be recovered from G' by applying a vertex splitting move at v which introduces the new vertex w.

The contraction move for a contractible FF edge need not preserve $(3,6)$-tightness, and therefore membership in the class $\mathcal{T}$. However we obtain in this section a key lemma which shows that when this occurs there exists a critical separating cycle, in the sense below, and an associated graph division $G \to \{G_1, G_2^\circ\}$, where $G_1 \subseteq G$ is a graph in $\mathcal{T}$.

Definition 4.1. An *annulus graph* A is a planar subgraph of the graph of a triangulated disc D which is obtained by the removal of the interior edges of a triangulated subdisc $D_1 \subseteq D$. Such a graph has an inherited facial structure and the cycles ∂D and ∂D_1 are the *boundary cycles* of A.

With this terminology, and in analogy with the notion of an embedded triangulated disc graph $i(D)$ in a torus graph G, we define an *embedded triangulated annulus graph* in G to be one of the form $i(A)$ where A is an annulus graph and i is injective on facial 3-cycles. We refer to such a subgraph as an *annular subgraph*. In particular we shall see that G_2° is an annular subgraph.

4.1. **Critical separating cycles.** Let G be a torus with hole graph with triple (T, D, i) and let c be a closed path of edges in G. Then c is said to be a *hole separating cycle* or simply a *separating cycle* if the context is clear, if there is a subgraph $G_1 \subseteq G$ which is a torus with hole graph with triple (T, D_1, i_1), where $D \subseteq D_1$, and c is equal to $i_1(\partial D_1)$ viewed as a path of edges. In the case of a noninjective detachment map with repeated edges the path c may be viewed more properly as a *directed* cycle in which, for a chosen orientation, no directed edges are repeated.

A separating cycle c gives a *division move* $G \to \{G_1, G_2^\circ\}$ where G_1 is the torus with hole graph defined by a triple (T, D_1, i_1), and G_2° is the annular subgraph determined by c and the faces of G which are not faces of G_1.

Definition 4.2. Let $G \in \mathcal{T}$.
(i) A separating cycle for G is a *critical separating cycle* if the graph G_1 for the associated division move $G \to \{G_1, G_2^{\circ}\}$ is $(3, 6)$-tight.

(ii) A *fission move* $G \to \{G_1, G_2\}$ for G is obtained from a critical separating cycle division $G \to \{G_1, G_2^{\circ}\}$ by attaching to G_2° the small graph H_i (given by Lemma 3.2) whose detachment map α_i is identified with the detachment map of G_1.

We shall see, in Lemma 4.5 that in all cases the graph G_2 is simple and $(3, 6)$-tight and so the resulting graphs of a fission move both lie in $\mathcal{T}$.

Note that critical separating cycles have length 9 and the annular graph G_2° has 2 boundary cycles of length 9. Also we note in Figure 10 that G_2° need not be a planar graph.
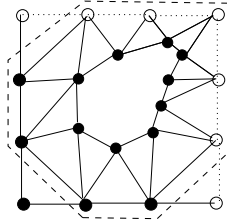

FIGURE 10. A critical separating cycle (dashed) with nonplanar annular graph G_2°.

The following "filling in" lemma will be useful for the analysis of critical separating cycles. It may be paraphrased as the assertion that a $(3, 6)$-tight subgraph of a graph $G \in \mathcal{T}$ contains no holes on its surface, bounded by 4 or more edges, which do not contain the superficial hole of G.

Lemma 4.3. *Let $G \in \mathcal{T}$ and let H be an embedded triangulated disc graph in G.*
(i) If K is a $(3, 6)$-tight subgraph of G with $K \cap H = \partial H$ then ∂H is a 3-cycle graph.
(ii) If K is a $(3, 6)$-sparse subgraph of G with $f(K) = 7$ and $K \cap H = \partial H$ then ∂H is either a 3-cycle or 4-cycle graph.

Proof. (i) The embedded assumption means that H is determined by a simplicial map from a triangulated disc to the simplicial complex for G with the property of being injective on 2-simplexes. Let us write H^c for the subgraph of G which contains the edges of ∂H and the edges of G not contained in H. Since $G = H^c \cup H$ and $H^c \cap H = \partial H$ we have

$$6 = f(G) = f(H^c) + f(H) - f(\partial H).$$

Since $f(H^c) \geq 6$ we have $f(H) - f(\partial H) \leq 0$. On the other hand,

$$6 \leq f(K \cup H) = f(K) + f(H) - f(\partial H)$$

and $f(K) = 6$ and so it follows that $f(H) - f(\partial H) = 0$.

Let $H = i(D)$, where D is a triangulated disc, and i is the embedding map. Since i is injective on the set of interior vertices of D and the set of interior edges of D, it follows that

$$f(H) - f(D) = f(\partial H) - f(\partial D).$$

We deduce that $f(D) - f(\partial D) = 0$. Since D is a triangulated disc this is only possibly if ∂D is a 3-cycle. Thus ∂H must also be a 3-cycle graph.

(ii) The argument above leads to $-1 \leq f(H) - f(\partial H)$ and hence to the inequality $-1 \leq f(D) - f(\partial D)$. This implies that ∂H is either a 3-cycle or 4-cycle graph. □

4.2. **Contraction and fission.** We now give a key lemma, Lemma 4.4, which will be used for the deconstruction and construction of graphs in $\mathcal{T}$. The following terminology will be useful.

Two facial 3-cycles of a torus graph are *adjacent* if they have a common edge. An edge of a subgraph K of a torus graph is a *boundary edge* if at most one of its facial 3-cycles is a subgraph of K, and the *boundary* ∂K of K is the graph determined by its boundary edges.

Lemma 4.4. *Let $G \in \mathcal{T}$, let e be a contractible FF edge in G, and let G' be the simple graph arising from the contraction move $G \to G'$ associated with e. Then either $G' \in \mathcal{T}$ or the edge e lies on a critical separating cycle.*

Proof. Let (T, D, i) be a defining triple for G and suppose that $G' \notin \mathcal{T}$. Note that the Maxwell count is preserved on contraction of the edge e and so G' must fail the $(3, 6)$-sparsity count. Thus there exists a subgraph K of G containing e for which the edge contraction results in a graph K' satisfying $f(K') < 6$.

Let $e = vw$ and let c and d be the facial 3-cycles which contain e. Note that if both c and d are subgraphs of K then $f(K) = f(K') < 6$, which contradicts the sparsity count for G. Thus K must contain either one or neither of these facial 3-cycles.

Suppose first that K is a maximal subgraph among all subgraphs of G which contains the cycle c, does not contain d, and for which contraction of e results in a graph K' which fails the $(3, 6)$-sparsity count. Note that $f(K) = f(K') + 1$ which implies $f(K) = 6$ and $f(K') = 5$. In particular, K is $(3, 6)$-tight, and is a connected graph.

Consider now an embedding of T on a topological torus. This provides a topological embedding of K determining a closed set $X(K)$. Also K has faces inherited from the facial structure of G and we let $\tilde{X}(K)$ be the union of $X(K)$ and the embeddings of these faces of K. Let $U_1, \ldots, U_k$ be the maximal connected open sets of the complement of $\tilde{X}(K)$ in the topological torus. Note that one of these open sets, U_1 say, contains the topological hole of G which, more precisely, is the complement of the closed set $\tilde{X}(G)$. There are two possible cases. For the first case each U_i is homeomorphic to an open unit disc. In the second case some U_i contains a curve which is not homotopic on the torus to a point. However, in the second case it follows that K is a planar graph, since it can be embedded in the complement of U_i. This is then a contradiction, since the edge contraction of a contractible FF edge in a planar triangulated graph preserves $(3, 6)$-sparsity. Thus each set U_i is the interior of the closed set determined by an embedded triangulated disc graph, say $H(U_i)$. (Indeed, the facial 3-cycles defining $H(U_i)$ are those whose torus embedding have interior set contained in U_i.) It follows that we may apply the filling in lemma, Lemma 4.3, to see that $\partial H(U_i)$ is a 3-cycle for $i > 1$. By the maximality of K, we have $k = 1$ (since adding the edges and vertices of T interior to these nonfacial 3-cycles gives a subgraph of G with the same freedom count). Thus, K is a subgraph of G determined by a hole separating cycle, namely the boundary cycle for $\partial H(U_1)$. This cycle is a critical separating cycle for G and so the proof is complete in this case.

It remains to consider the case for which K contains neither of the facial 3-cycles which contain e. Thus $f(K) = f(K') + 2$ and $f(K) \in \{6, 7\}$. Once again we assume that K is a maximal subgraph of G with respect to these properties and consider the complementary components $U_1, \ldots, U_k$. As before each set U_i is homeomorphic to a disc and determines an embedded triangulated disc graph $H(U_i)$, one of which, say $H(U_1)$, contains the graph $i(D)$. The filling in lemma and maximality now implies that each boundary of $H(U_i)$, for $i > 1$, is a 4-cycle. By the maximality of K, we see once again that $k = 1$ (since adding the missing edge for such a 4-cycle gives a subgraph of G with a lower freedom count) and the proof is completed as before.   □

We now show that the move $G \to \{G_1, G_2\}$, associated with a critical separating cycle, is indeed a fission move in the class $\mathcal{T}$.

Lemma 4.5. *Let $G \to \{G_1, G_2^\circ\}$ be a division move associated with a critical separating cycle whose detachment map has associated graph H_i. Let $G_2 = H_i \cup G_2^\circ$ be the torus with hole graph obtained by substituting H_i for G_1 in the graph G. Then G_2 is simple and $(3, 6)$-tight.*

Proof. Let A be the annular graph G_2°. Then the graph intersections $G_1 \cap A$ and $H_i \cap A$ coincide. Also we have

$$6 = f(G) = f(G_1 \cup A) = f(G_1) + f(A) - f(G_1 \cap A) = 6 + (f(A) - f(H_i \cap A))$$

Thus $f(A) - f(H_i \cap A) = 0$ and so

$$f(G_2) = f(H_i) + f(A) - f(H_i \cap A) = 6.$$

It remains to show that G_2 is simple and $(3, 6)$-sparse. If G_2 is not simple then, since A and H_i are simple there is an edge e of H_i with the same vertices as an edge f of A. Also these vertices belong to the critical separating cycle. But then $G_1 \cup \{f\}$ is a subgraph of G with freedom count 5 which is a contradiction.

To determine the sparsity of G_2 let K be a subgraph of the graph $G_2 = H_i \cup A$ with at least 3 vertices. Then

$$f(G_1 \cup (K \cap A)) = f(G_1) + f(K \cap A) - f(G_1 \cap A \cap K)$$

from which it follows that $f(K \cap A) - f(G_1 \cap A \cap K) \geq 0$, since G is $(3, 6)$-sparse and $f(G_1) = 6$. On the other hand

$$G_1 \cap A \cap K = H_i \cap A \cap K$$

and so

$$f(K) = f(K \cap H_i) + f(K \cap A) - f(H_i \cap A \cap K) \geq f(K \cap H_i)$$

Thus $f(K) \geq 6$ (as desired) except possibly in the case that $K \cap H_i$ consists of a single edge. If this edge is an edge of the boundary cycle then K is a subgraph of G and it follows immediately that $f(K) \geq 6$. So the final case to consider is the case $K = K_1 + e$ where K_1 is a $(3, 6)$-tight subgraph of A which meets H_i at 2 vertices, being the vertices of a nonboundary edge e of H_i. We next show that this does not occur by making use of the filling in lemma.

As in the previous proof we consider representations of torus with hole graphs on a topological torus, $[0, 1]^2/ \sim$, given through a representation on the closed unit square

$[0,1]^2$. Also we will consider subsets of this torus determined by the given facial structure on the graphs.

First, represent G on $[0,1]^2/\sim$ so that the critical separating cycle, c say, which is associated with the division $G \to \{G_1, G_2^{\circ}\}$, is represented by a simple closed curve γ in $[0,1]^2$, marked with the vertices of c. (As usual the structure of c is reflected in the way in which γ meets the boundary of $[0,1]^2$ and some vertices may be marked on opposite points of this boundary.) It follows that the annular graph $A = G_2^{\circ}$ is represented by the embedding in $[0,1]^2$ of the triangulated annulus graph associated with A.

The graph G_2 is defined through a substitution of G_1 by the graph H_i and it too has a division $G_2 \to \{H_i, A\}$ determined by c. Also G_2 has a representation on $[0,1]^2/\sim$ which agrees with the representation of G on the common subgraph A.

Consider now the subgraph $K_1 \subset A$. We denote the vertices of the edge e, as x and y.

The edges of K_1 determine a closed subset $X(K_1)$ of the torus and the edges and faces (ie facial 3-cycles) of K_1 determine the closed set $\tilde{X}(K_1)$. The open subset of the torus determined by the intersection of the interior of γ and the complement of $\tilde{X}(K_1)$ contains at least two connected component regions. One of these corresponds to or contains the hole of G. (The hole of G is represented in the torus as the interior of the set $\tilde{X}(D)$ for the triangulated disc D associated with G.)

Figure 11 depicts an example of the representation γ in $[0,1]^2$ and subsets which correspond to $\tilde{X}(K_1)$ and these regions (and labelled accordingly). The simple curve representing the edge e is not depicted. In general this will be a curve exterior to γ with initial and final points carrying the labels x and y (for which there may be choices), and the curve may have several components corresponding to transits through opposing boundary points.
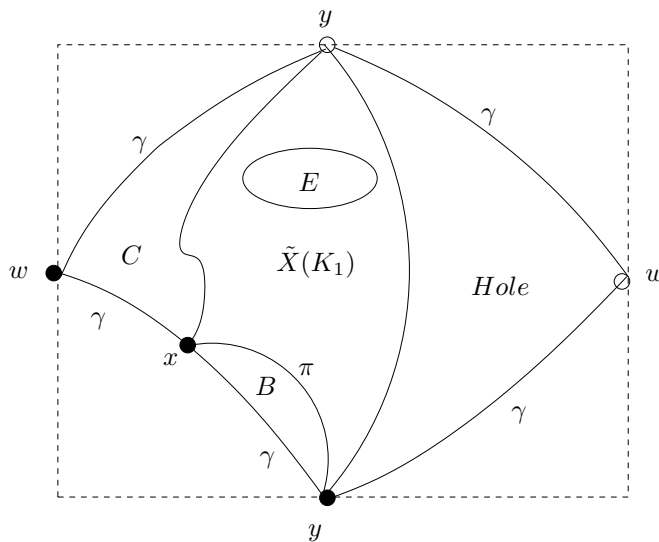

FIGURE 11. Regions of $[0,1]^2$ corresponding to the regions of the torus $[0,1]^2/\sim$ associated with γ and K_1.

Since K_1 and G_1 are $(3,6)$-tight the subgraph $G' = G_1 \cup K_1$ of G is $(3,6)$-tight and the intersection of K_1 and G_1 consists of the 2 vertices of e, denoted x and y. The filling in lemma, Lemma 4.3, applies to G' and we deduce that the boundary curve of each of the non hole regions of the torus (such as B, C and E etc.) represents a 3-cycle subgraph of G. (Specifically, the role of the subgraph K in that lemma is played by G' and the role of the embedded triangulated disc graph H is played by the subgraph corresponding to one of the non hole-containing regions of the torus.)

Consider the curve π from y to x which lies in the boundary of $\tilde{X}(K_1)$ and the boundary of one of the regions indicated above on the torus. If this region is not the hole-containing region (for the hole region associated with G) then it corresponds to a subpath p of a 3-cycle. If p has length 1 then adding the corresponding edge to G_1 gives a subgraph of G with freedom count 5 which is a contradiction. On the other hand if the length of p is 2 then the edge e lies in c and adding this edge to K_1 gives a subgraph of G with freedom count 5, and so this again is a contradiction. Since there is at least one region that does not contain the hole region for G the proof is complete. $\qquad\square$

We now deduce that there is a *contraction fission sequence* for any graph $G \in \mathcal{T}$ as described in the next corollary.

Note that the boundary cycle $i(D)$ determined by the triple (T, D, i) for G is a critical separating cycle which is *improper* in the sense that $G_1 = G$ and G_2° is equal to c as a graph. We say that c is *proper* if it is not improper. Also we note in Figure 10 a proper critical separating cycle c_1 need not provide a fission move with the property, which we call the *reducing property*, that G_2 is smaller than G in the sense of having fewer faces. However, we now show that if there is a *proper* critical separating cycle then there is a contraction move in the class $\mathcal{T}$ or there is a critical separating cycle with the reducing property. The corollary then follows readily from this fact and the key lemma.

Suppose then that c is a proper critical separating cycle for $G \in \mathcal{T}$. Then G_2° contains a face of G with an edge xy on c and third vertex $z \in G_2^\circ$. Also z has degree 3 or more, since G is $(3,6)$-tight. Since G_2° is an annular graph it follows that there is an FF edge e in G_2° with both faces in G_2°. If contraction of e yields a graph in $\mathcal{T}$ then this edge contraction may be used for the reduction scheme in the corollary. So we may assume that this is not the case. By the key lemma, either there is a critical separating cycle c' though e or the edge e lies in a non facial 3-cycle of G_2°. In the latter case G_2° contains the graph of a triangulate disc (all of whose faces are faces of G) whose outer boundary is the non facial 3-cycle. It is well-known that such a graph (a triangulated sphere) has an edge f of FF-type whose contraction is simple graph (see Section 5.2 of [3] for example) and so f can play the role of e in this case. We can also assume that c' lies in G_2°. To see this note first that if c, c' are oriented critical cycles for G with source vertex v and the same orientation (relative to the hole), and if π, π' are subpaths with initial vertex v and common final vertex w, then necessarily π, π' have the same length. (If not then a substitution between π and π' creates a critical separating directed cycle of length less than 9.) In view of this principle, if c, c' have common vertices then we may substitute such a subpath of π' containing e for its corresponding subpath π to obtain a critical cycle in G_2°. (If c, c' do not have a common vertex then c' already lies entirely in G_2°.) It now follows that the division move for c' produces an annular graph with fewer faces than G_2°.

Definition 4.6. A torus with hole graph is *uncontractible* if it has no FF edges or if every edge of type FF lies on a nonfacial 3-cycle.

Corollary 4.7. *Let G be a torus with hole graph in $\mathcal{T}$. Then there exists a finite rooted tree in which each node is labelled by an element of $\mathcal{T}$ such that,*

  (i) *the root node is labelled G,*
 (ii) *every node has either one child which is obtained from its parent node by an FF edge contraction, or, two children which are obtained from their parent node by a fission move for a critical separating cycle,*
(iii) *each leaf is an uncontractible graph.*

$$G \longrightarrow G_1 \nearrow \begin{array}{c} G_{11} \longrightarrow G_{111} \\ \\ G_{12} \end{array} \nearrow \begin{array}{c} G_{121} \\ \\ G_{122} \longrightarrow G_{1221} \end{array}$$
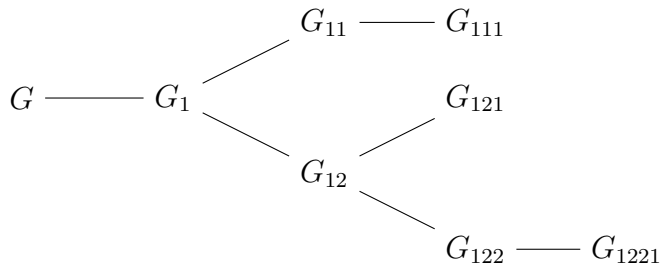
FIGURE 12. Contraction and fission to uncontractible graphs in $\mathcal{T}$.

The inverse move for edge contraction in the class $\mathcal{T}$ is a vertex splitting move, which as we have noted, preserves 3-rigidity. Also the inverse of a fission move, which we refer to as a *fusion move*, corresponds to substitution of the subgraph H_i of G_2 by the graph G_1. It is immediate from the definition of infinitesimal rigidity that if G_1 and G_2 are 3-rigid then so too is G. A proof of the equivalence of (i) and (ii) in the main theorem can therefore be completed by showing, as we do in the next section, that the uncontractible graphs in $\mathcal{T}$ are 3-rigid.

5. The rigidity of uncontractible graphs

We now show that the uncontractible graphs of $\mathcal{T}$ are 3-rigid. This completes our first proof of the equivalence of (i) and (ii) in the main theorem.

This will be achieved in two steps. The first step shows that uncontractible graphs G in $\mathcal{T}$ have no *interior vertex*. This means that each vertex of G lies on ∂G, and so, in particular, $|V(G)| \leq 9$. This leads quickly to the fact that the uncontractible graphs with at most 8 vertices are 3-rigid. In the second step we show that the graphs with 9 vertices and no interior vertices are contractible.

Lemma 5.1. *Let $G \in \mathcal{T}$ be an uncontractible graph. Then the interior vertices of G have degree at least 6.*

Proof. A vertex v is an interior vertex if and only if all edges incident to v are of FF type. Since G is $(3, 6)$-tight it contains no vertices of degree 1 or 2. If $\deg(v) = 3$ then it follows from the simplicity of G that each of the three edges incident to v does not lie on a non-facial 3-cycle. This contradicts the uncontractibility of G. If v has degree 4 then the induced subgraph $X(v)$ for v and its 4 neighbours has at least 10 edges. These are the 8

edges for the faces incident to v and at least 2 further edges to fulfil the uncontractibility condition. Thus $f(X(v)) \leq 5$ which is contrary to G being $(3,6)$-tight. One can similarly check that $f(X(v)) \leq 5$ if the degree of v is 5. $\square$

The proof of the next lemma exploits the topological nature of the torus. For this and subsequent arguments it is convenient to define the homology class of an FF edge e in the case that $e = xy$ with $x, y \in \partial G$ and $e \notin \partial G$. We refer to refer to such an edge as a *crossover edge*.

Definition 5.2. Let G be a torus with hole graph with triple (T, D, i), let e be a crossover edge and let $\tilde{e}$ be any directed cycle of edges formed by e and a path of edges from ∂G. The *homology class* of e is the unordered pair $\{[\tilde{e}], -[\tilde{e}]\}$ associated with the homology class $[\tilde{e}]$ in $H_1(T, \mathbb{Z})$ of the cycle $\tilde{e}$.

The homology class of a crossover edge e is well defined and not equal to the trivial homology class. For simplicity we write $[\tilde{e}]$ for the homology class of e. In Figure 13 we indicate the partitioning of the crossover edges of the graph H_1 according to homology class.
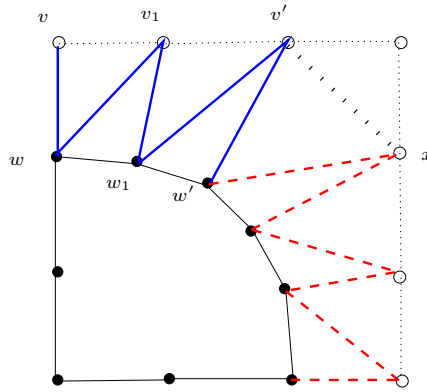
FIGURE 13. The 12 crossover edges of the graph H_1 fall into 3 homology classes.

The limited possibilities for the classes $[\tilde{e}]$ become apparent on considering G as an embedded graph on the topological torus. In the case of boundary type $9v$ the boundary graph edges determine a simple closed curve, γ say. If there are no interior vertices then the curves for the remaining edges are disjoint except possibly at their endpoints on γ. In view of this disjointness it follows that there can be at most *three* distinct homology classes for such edges. Indeed, Figure 14 indicates three embedded crossover edges. (With respect to a natural identification of the homology group with $\mathbb{Z}^2$ these have homology classes $(1, 0)$, $(0, 1)$ and $(1, 1)$, up to sign.) Note that no further homology class is possible for any additional embedded FF edge. The figure illustrates the embedding of a $9v$ type graph but in fact the argument is the same in general, when γ may have points of self contact.
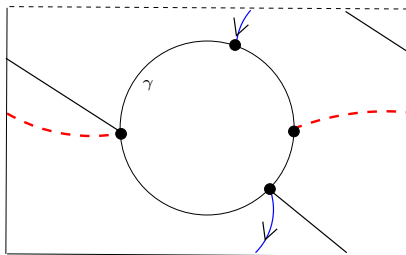
FIGURE 14. A representation of 3 embedded edges of FF type with different homology classes.

Lemma 5.3. *Let $G \in \mathcal{T}$ be an uncontractible graph. Then G has no interior vertices.*

Proof. Let (T, D, i) be a triple associated with G. Let $v_1, v_2, \ldots, v_r$ be the neighbours of an interior vertex z written in order, so that $zv_1v_2, zv_2v_3, \ldots$ are facial 3-cycles of G. By the uncontractibility of G for each vertex v_i the edge zv_i lies on a non-facial 3 cycle and so there is an additional edge v_iv_j for some $j \neq i - 1, i + 1$.

Suppose first that the degree of z is 6. Then the subgraph $X(z)$ induced by z and its neighbours includes the 6 edges incident to z, the 6 perimeter edges v_iv_{i+1} and additional edges between non adjacent perimeter vertices $v_1, \ldots, v_6$. There are at least 3 such edges, and since $f(X(z)) \geq 6$ it follows that there are exactly 3, say e_1, e_2, e_3. Let $\tilde{e}_1, \tilde{e}_2, \tilde{e}_3$ be choices of 3 non-facial 3-cycles for the edges e_1, e_2, e_3 and let $[\tilde{e}_1], [\tilde{e}_2], [\tilde{e}_3]$ be the associated homology classes in $H_1(T, \mathbb{Z})$.

Figures 15, 16 show two examples of such a graph $X(v)$ embedded on a topological torus $S^1 \times S^1$. For an appropriate identification of $H_1(T, \mathbb{Z})$ with $\mathbb{Z}^2$ the homology classes $[\tilde{e}_1], [\tilde{e}_2], [\tilde{e}_3]$ in these examples are

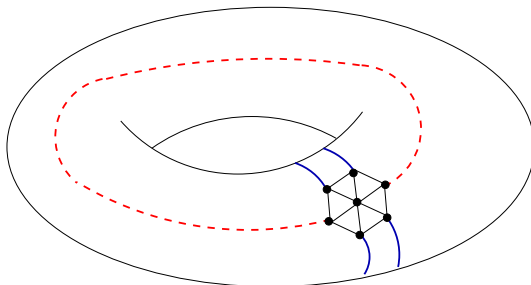$$(1, 0), (1, 0), (0, 1) \quad \text{and} \quad (1, 0), (0, 1), (1, 1).$$

FIGURE 15. An embedding of a subgraph $X(z)$.

Consider the maximal connected open subsets R of $S^1 \times S^1$ that are complementary to $X(z)$ as an embedded graph. We refer to these relatively open sets as *regions*. Examining rectangular representations of the embedded graph we see that in the first example there are two non-facial regions, one of which is bounded by a directed 4-cycle of embedded edges
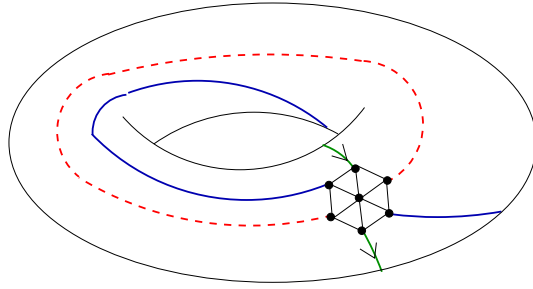
FIGURE 16. An embedding of subgraph $X(z)$.

and one of which is bounded by a directed 8-cycle, and there are 6 regions for the facial 3-cycles of $X(v)$. This also holds for the case of a homology class triple $(1,0),(1,1),(1,1)$.

In the example of Figure 16, with homology triple $(1,0),(0,1),(1,1)$ there are two non-facial regions each of which is bounded by an embedded 6-cycle. Thus in both cases that the nonfacial regions are bounded by $4,6$ or 8 edges.

The remaining case in which the homology classes $[\tilde{e}_1],[\tilde{e}_2],[\tilde{e}_3]$ coincide cannot occur since G is a simple graph without loops and the embedded edges for e_1, e_2, e_3 are disjoint except at their endpoints.

Consider now the embedded graph for the containing torus graph T for G. Note that each of the non-facial regions R defines a subgraph G_R of T which is a torus with hole graph whose boundary corresponds to the boundary of the region. In view of the observations on boundary lengths, each graph G_R has freedom number $f(G_R) < 6$. However, one of these graphs is a subgraph of G, and this contradicts the $(3,6)$-sparsity count for G. So we conclude that G has no interior vertices of degree 6.

Suppose now that $\deg(z) = 7$. We may view $X(z)$ in this case as arising from the $\deg(z) = 6$ case by the addition of a new vertex v_* between v_i and v_{i+1}, with the edge $v_i v_{i+1}$ replaced by two edges $v_i v_*, v_* v_{i+1}$ and with the edge $z v_*$ added. Moreover an embedded graph in the degree 6 case can be augmented in a corresponding way to provide the embedded graph for the degree 7 case. By the uncontractibility of G there is an edge $v_* v_j$ for some j which is embedded and we see that its embedding divides an r-cycle region (for the degree 6 case) into two regions. Moreover it follows that the boundary cycles for these regions do not use more edges. Thus we obtain a contradiction as before. By induction the same conclusion holds in general and so G has no interior vertices of degree n for all $n \geq 6$. In view of Lemma 5.1 there can be no interior vertices of any degree. $\qquad\square$

Recall that the double banana graph, G_{DB} say, is formed by joining two copies of the (single banana) graph $K_5 \backslash e$ at their degree 3 vertices. Evidently this graph is $(3,6)$-tight and fails to be 3-rigid and it is well known that this is the only graph with 8 or fewer vertices with this property. The next lemma combined with the previous lemma shows that the uncontractible graphs with 8 or fewer vertices are 3-rigid.

Lemma 5.4. *Let $G \in \mathcal{T}$ be a graph in $\mathcal{T}$ with no interior vertices and no more than 8 vertices. Then G is 3-rigid.*

Proof. It suffices to show that if G has 8 vertices then it is not equal to G_{DB}. Since G and ∂G have the same vertex set it follows that the boundary graph is of type $v3v6$ or $v4v5$.

Considering an embedded graph representation of G in a torus $R/\sim$, with the detached disc represented by an open subset of R, it follows that in fact any torus with hole graph with this form of boundary is 3-connected. Since the double banana graph is not 3-connected the proof is complete. $\square$

We now embark on showing the remaining case (step 2) that the graphs G in $\mathcal{T}$ with boundary type $9v$ and no interior vertices are contractible. It is possible to give a rather extended ad hoc embedded graph argument to show this, and in fact this method is employed in Section 5 for a range of small graph types. However we now give a more sophisticated proof, exploiting once again the homology classes of edges, and which provides some general methods and other insights.

The main idea may be illustrated by considering again the 9 vertex graph H_1, labelled as in Figure 13. The edges vw and $v'w'$ are FF edges of the same homology class, as are the 3 "intermediate v to w edges". We note that the "interior edge" v_1w_1 (in contrast to $v'w_1$) does not lie on a nonfacial 3 cycle. Also it can be shown that it does not lie on a critical separating cycle, and so the graph is reducible in $\mathcal{T}$ by edge contraction. In general we will identify such edges within subgraphs (called panel subgraphs) determined by crossover edges of the same homoloy class.

First we note two general lemmas that ensure contractibility. (These lemmas also play a role in the ad hoc arguments in Section 5.)

Lemma 5.5. *Let G be a graph of $\mathcal{T}$ with a degree 3 vertex on the boundary graph ∂G which is incident to an FF edge e. Then the graph obtained from the contraction of e is in $\mathcal{T}$.*

Proof. That the contracted graph is $(3,6)$-tight follows from the fact that subtracting v and its 3 incident edges from a subgraph does not change the freedom number. Also it is elementary to check that the contracted graph is a torus with hole graph. $\square$

Lemma 5.6. *Let $G \in \mathcal{T}$ with $V(G) = V(\partial G)$ and let c be a critical cycle of edges which is not the detachment map cycle for G. Then there is an edge contraction of G to a graph in $\mathcal{T}$.*

Proof. Let π be the directed 9-cycle for the detachment map of G. Then c and π form the boundary of an annular subgraph H of G and we assume that they have the same orientation. Let x be a vertex such that the edges $e = xy, f = xw$ are edges of π and c which start at x, with $e \neq f$, and such that there are subpaths π_1, c_1 of the critical cycles from x to a common vertex z. We may also assume that z is the first such vertex. Thus the subpaths form the boundary of either a facially triangulated disc, if $z \neq x$, or, if $z = x$, a triangulated disc with two boundary vertices identified. We denote this subgraph of H as H_1. See Figure 17.

The subpaths π_1, c_1 are of the same lengths, say r, since π and c are critical separating cycles, and the triangulation is formed by the addition of edges only. It follows by elementary graph theory that there is a degree 3 vertex u strictly between x and z on the subpath π_1. Indeed, the graph H_1 has exactly $2r - 2$ bounded faces from the triangulation by facial 3-cycles of G. If the degrees of the intermediate vertices u are greater than 3 then there would be at least $2(r-1) + 1$ faces incident to these vertices.

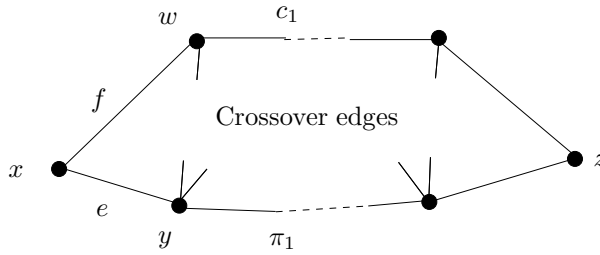Since the vertex u is incident to an FF edge the previous lemma applies to complete the proof. □

FIGURE 17. Subpaths of c and π from x to z.

We now define *panel subgraphs* of a graph $G \in \mathcal{T}$ with $|V(G)| = |V(\partial G)| = 9$, and show that their strongly interior edges (defined below), should they exist, allow contraction to a graph in $\mathcal{T}$.

Consider two distinct crossover edges $e = vw, e' = v'w'$ which have the same homology class. They determine a triangulated disc subgraph of G, and its containing torus graph T, which may be visualised as a planar *triangulated panel* of G. The vertex set consists of the vertices of e, e', of which there are 3 or 4 in number, and vertices on the hole boundary lying on two paths, between v and v' and between w and w'. Figure 18 indicates such a panel subgraph with 5 faces.
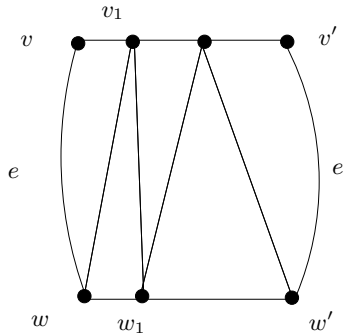
FIGURE 18. A panel subgraph of G determined by two crossover edges e, e' of the same homology class.

Considering embedded graphs in the torus it follows readily that every panel graph is contained in a unique maximal panel subgraph.

Note that the *interior vertices of the panel*, that is, those without incidence with e or e', are only incident to edges of the panel subgraph. It follows that any *strongly interior edge* v_1w_1 of such a panel, that is, one with both v_1 and w_1 interior vertices, does not lie on a nonfacial 3-cycle.

Note that Lemma 5.6 implies that if G is not contractible to a graph in G then there can be no critical separating cycles. Thus, in view of the previous paragraph, there can be no strongly interior edges of the panel if G is not contractible to a graph in $\mathcal{T}$.

Lemma 5.7. *Let G be a graph in $\mathcal{T}$ with $|V(G)| = |V(\partial G)| = 9$. Then G may be contracted to a graph in $\mathcal{T}$.*

Proof. By the previous discussion we may assume that the maximal panel subgraphs do not have a strongly interior edges. Also, by Lemma 5.5, we can assume that there are no vertices in G of degree 3. It follows that each such subgraph has at most 4 crossover edges. Since there are 12 crossover edges, by $(3,6)$-tightness, and at most 3 crossover edge homology classes, it follows that there are 3 panels, each with 4 crossover edges. Thus the panel subgraphs have the form indicated in Figure 19.
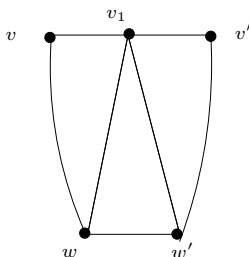
FIGURE 19. A panel subgraph with 4 crossover edges and no interior degree 3 vertex.

By Lemma 5.6 we may assume that every crossover edge is not on a critical cycle. However, we now show that this is not possible, completing the proof.

Consider a single pair of interior edges, v_1w, v_1w' on one of the panel graphs. These edges and their panel subgraph are illustrated in the embedded graph diagram of Figure 20. If v_1w lies on a nonfacial 3-cycle then this is achieved through edge v_1v' of the panel and one of the 8 remaining crossover edges with a different homology class. This crossover edge from v to w is indicated in the figure with label g. Note however, that if g' is another embedded edge of the same homology type as g then, from the disjointness requirement for embedded edges, g' has the form $v'x$ (or the form yw), where x (resp. y) lies on the hole boundary arc from v to w (resp. v' to w') as indicated in the figure. It follows that the form of the panel for this homology type cannot hold, and this contradiction completes the proof. $\qquad \square$

6. VERTEX SPLITTING CONSTRUCTION

We now obtain an alternative proof of the equivalence of (i) and (ii) in the main theorem. Also we determine exactly the uncontractible graphs in $\mathcal{T}$ and with this we complete the proof of the equivalence of (i), (ii) and (iii).
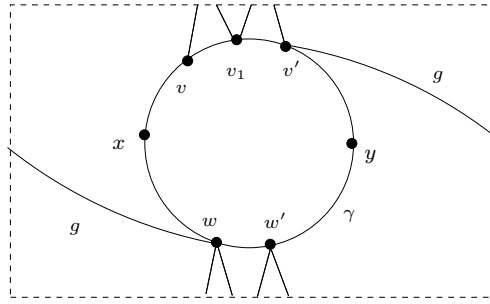
FIGURE 20. Only edges of the form xv' or vy have the same homology type as the edge g.

Lemma 6.1. *Every graph in $\mathcal{T}$ admits a contraction sequence in $\mathcal{T}$ to an uncontractible graph.*

Proof. Let $G \in \mathcal{T}$ and suppose that G is a contractible torus with hole graph. We show that there exists a contractible edge for which the contraction yields a graph in $\mathcal{T}$.

Since G is contractible there exists an FF edge which is not on a nonfacial 3-cycle. If the contracted graph is in $\mathcal{T}$ we may continue the argument with a smaller graph. So we may assume, by the critical cycle lemma, Lemma 4.4, and the discussion preceding Corollary 4.7, that there exists a proper critical cycle c_1 and an associated division $G \to \{G_1, G_2^\circ\}$ where G_1 is in $\mathcal{T}$ and both G_1 and the annular graph G_2° have fewer vertices than G. Since G_2° contains a face of G it follows, again by the discussion preceding Corollary 4.7 that the annular graph contains an edge e of FF type.

We may assume, moreover, that the edge e does not lie on a nonfacial 3-cycle. To see this we note the two possibilities that hold if e does lie on a nonfacial 3-cycle. Either the 3-cycle is triangulated by faces of G, or the triangulation of the 3-cycle in the containing torus graph for G contains the associated triangulated disc for the detachment map for G. In the latter case it follows that G contains a fully triangulated torus graph, which violates $(3, 6)$-sparsity, and so this case does not occur. In the former case G contains the graph of a triangulated sphere all of whose faces are faces of G. Such graphs have edges which are of FF type and do not lie on a nonfacial 3-cycle, and so we may rechoose e to be such an edge.

Since the annular graph contains an edge of FF type which is not on a nonfacial 3-cycle we may either contract with this edge to a smaller graph in $\mathcal{T}$ or, by the critical cycle lemma, obtain another proper critical cycle, c_2 say, and an associated division $G \to \{H_1, H_2^\circ\}$ with $H_1 \in \mathcal{T}$, where these graphs have fewer vertices than G.

Note that we can assume that c_2 lies inside c_1, or, more precisely, that the detached triangulated disc for c_2 is contained in the detached triangulated disc for c_1. One way to see this is to note that the union J of G_1 and H_1 is a proper subgraph of G which lies in $\mathcal{T}$. Thus we may replace c_2 by the proper critical cycle for the detachment map for J. By the reasoning above there is a contractible edge in the associated annular graph which does not lie on a nonfacial 3-cycle.

Repeating this process, identifying nested critical cycles $c_1, c_2 \ldots$, we must eventually obtain a contractible edge for which the contracted graph lies in $\mathcal{T}$. Indeed, if this did not

occur then the process provides an infinite strictly increasing sequence of proper subgraphs of G and this contradicts the finiteness of the graph. $\square$

We have shown that the uncontractible graphs in $\mathcal{T}$ are 3-rigid by the analysis in Sections 4 and 5. This, together with Lemma 6.1 provides a second proof of the equivalence of (i) and (ii) in the main theorem, which avoids the use of fission moves.

In fact we can obtain a stronger result by enlarging the analysis of the small graphs to identify the uncontractible graphs of $\mathcal{T}$.

Theorem 6.2. *The uncontractible graphs of $\mathcal{T}$ are the graphs H_{16} and H_{17}.*

To obtain this fact note first that H_{16} and H_{17} are uncontractible. Also it is straightforward to check, with the assistance of Lemmas 5.5 and 5.6, that the particular graphs $H_2, \ldots, H_{15}$ are contractible in $\mathcal{T}$, and indeed, are completely contractible in the class $\mathcal{T}$ to one of these two graphs. However, it remains to check that every graph with no interior vertices and one of these boundary types is similarly contractible. We show this in the second part of the Appendix by arguments which become progressively simpler as the number of vertices decrease.

Remark 6.3. It is natural to seek a combinatorial characterisation of 3-rigid torus with hole graphs along similar lines. Natural examples, which are not minimally 3-rigid, can be found amongst those graphs, G^+ say, which may be obtained by merging the boundaries of a $(3, 6)$-tight torus with hole graph G and an annular graph H with a 9-cycle boundary and an r-cycle boundary, where $4 \leq r \leq 8$. Here, of course, the identified directed 9-cycles for G and H should be of the same detachment type α_i, for some $1 \leq i \leq 17$. For such graphs G^+ there is a simple necessary and sufficient condition for 3-rigidity, namely that the annular graph should have girth r, meaning that there is no hole separating cycle c for G^+ which lies in H and has length less than r. We expect that an examination of the relevant small graphs will provide a basis for a proof that the graphs G^+ are precisely the 3-rigid torus with hole graphs.

7. APPENDIX

We first give the proof of Lemma 3.2.

Lemma 3.2. *There is a collection of graphs $H_1, \ldots, H_{17}$ in $\mathcal{T}$ with detachment maps $\alpha_i, 1 \leq i \leq 17$, and the following properties.*
(i) If $G \in \mathcal{T}$ with detachment map α then there is a unique graph H_i and a graph isomorphism $\phi : \partial G \to \partial H_i$ such that $\alpha = \phi \circ \alpha_i$.
(ii) $V(H_i) = V(\partial H_i)$, for each i.

Proof. The proof of the lemma follows the following scheme. We identify the detachment maps $\alpha_1, \ldots, \alpha_{17}$ that are possible for graphs in the class $\mathcal{T}$, arguing case by case for fixed values of $|V(\partial G)|$. These values range from 9 to the minimum possible value which turns out to be 4. At the same time we identify corresponding vertex minimal graphs $H_1, \ldots, H_{17}$ for these types.

Let $G \in \mathcal{T}$ be a $(3, 6)$-tight torus with hole graph with the attachment map α. The graphs H_1, H_2, H_3 and their detachment maps $\alpha_1, \alpha_2, \alpha_3$ have been described above. If $|V(\partial G)| = 9$ then $\alpha = \alpha_1$ while if $|V(\partial G)| = 8$ then either $\alpha = \alpha_2$ or $\alpha = \alpha_3$.

We next look at the case of 1 repeated edge which is the case $|V(\partial G)| = 7, |E(\partial G)| = 8$. The detachment map, and the boundary graph, evidently has at most one form, with cyclic word $e3e4$. An associated vertex minimal graph H_4 in $\mathcal{T}$ is defined by the rectangular face graph in Figure 21.
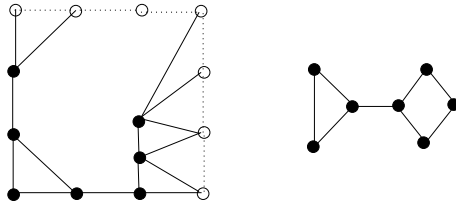

FIGURE 21. A rectangular face graph representation for the graph H_4, with boundary graph of type $e3e4$.

We next consider the case of graphs in $\mathcal{T}$ with

$$|V(\partial G)| = 7, \quad |E(\partial G)| = 9$$

Assume first that there are distinct vertices v, w in ∂G and 4 edge-disjoint consecutive paths of edges between them, from v to w, w to v, v to w and w to v, respectively, with lengths a, b, c, d say, so that the cyclic word type for the detachment map of α is $vawbvcwd$. Thus we are assuming that v and w alternate in the cyclic word. Figure 22 indicates how this may be depicted as an embedded cycle on a topological torus.
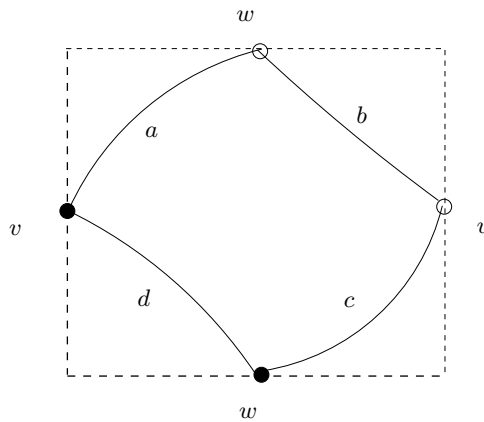
FIGURE 22. Boundary cycle of type $vawbvcwd$ with $a + b + c + d = 9$.

Since the graphs in $\mathcal{T}$ are simple it follows that the sum of any two of a, b, c, d is at least 3. In fact this is the only constraint and up to cyclic order and reversals there are 5 types for such quadruples (a, b, c, d), namely

$$(1, 2, 2, 4), (1, 2, 3, 3), (1, 2, 4, 2), (1, 3, 2, 3), (2, 3, 2, 2),$$

and there are 5 associated detachment maps, of types $v1w2v2w4$, etc. The graphs in Figures 23, 24 give representative vertex minimal graphs, $H_5, \ldots, H_9$ for these attachment types.
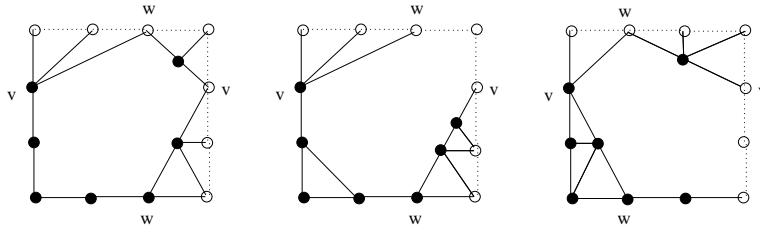
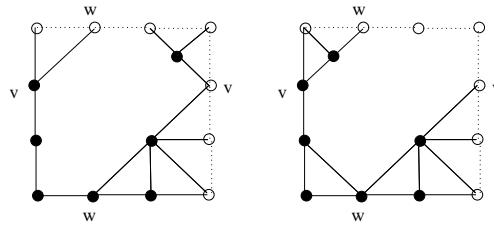FIGURE 23. Rectangular face graph representations for H_5, H_6, H_7.

FIGURE 24. Rectangular face graph representations for H_8, H_9.

We now look at the nonalternating case so that the cyclic word for the detachment map α is $vavbwcwd$. Since G is simple it follows that a and c are at least 3 and so there is a unique form up to relabelling and ordering, namely $v3v2w3w1$. (See Figure 25.)
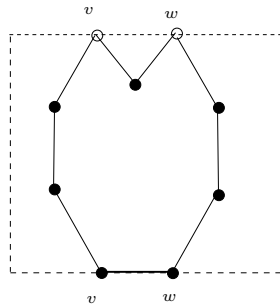
FIGURE 25. Boundary graph type $v3v2w3w1$.

In this case we see that G contains a triangulated sphere which is formed by the part of the triangulated torus for G which lies "between" the two nonfacial 3-cycles associated with the subwords $v3v$ and $w3w$. Moreover G contains the augmentation of this subgraph by the edge vw and so G cannot be $(3,6)$-tight. Figure 26 also indicates a perspective view of such a graph. Since G is assumed to be $(3,6)$-tight, this type of detachment map cannot occur.

There is one further case of a torus with hole graph with $|V(\partial G)| = 7, |E(\partial G)| = 9$. The detachment map is of type $v3v3v3$ and G can be thought of as a torus graph with a 6-cycle hole to which a triangle has been attached by a single vertex. In particular such graphs are not $(3,6)$-tight.

As an aside we remark that it follows from the main theorem that every graph in $\mathcal{T}$ is 3-connected. However, this fact may also be proved directly by an embedded graph argument analogous to the one used in the exclusion of the small graph in Figure 25.
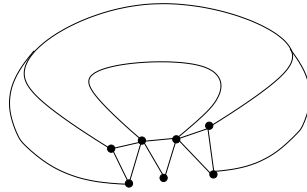

FIGURE 26. A torus with graph satisfying the Maxwell count $f(G) = 6$ which is not $(3,6)$-tight.

Consider now the possibility of a detachment map with 3 (pairwise) repeated vertices and no repeated edges, so that $|V(\partial G)| = 6$ and $|E(\partial G)| = 9$. There are 2 attachment map types given by the cyclic words $v1w2x1v2w1x2$ and $v1w1x1v2w2x2$ which are represented by the graphs H_{10}, H_{11} of Figure 27. In fact there are no other forms possible for graphs in $\mathcal{T}$ with this vertex and edge count for ∂G. Indeed, in analogy with the graph types of Figure 26, a torus with hole graph whose cyclic word contains disjoint subwords of the form $w1v$ and $v2w$ is not $(3,6)$-tight.
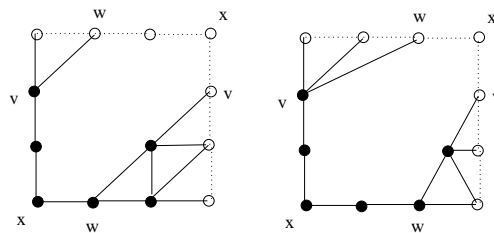

FIGURE 27. Face graphs for H_{10}, H_{11}, with types $v1w2x1v2w1x2$ and $v1w1x1v2w2x2$.

We next consider further types with fewer than 9 edges in the boundary graph. The first case to consider is
$$|V(\partial G)| = 6, \qquad |E(\partial G)| = 8.$$

In this case there are 3 types of detachment map, for simple torus with hole graphs, and these correspond to the cyclic words

$$v3e2v1e1, \quad v3e1v2e1, \quad v2e2v2e1$$

The structure of these words is depicted in Figure 28 and representative vertex minimal graphs in $\mathcal{T}$ are given in Figure 29.
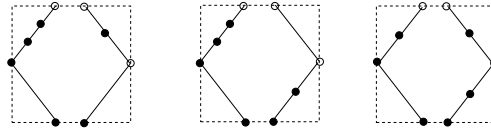

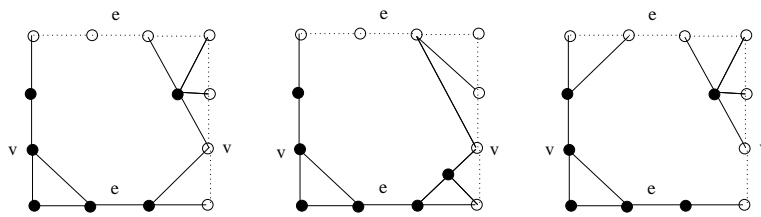FIGURE 28. Hole types $v3e2v1e1$ etc., for H_{12}, H_{13}, H_{14}

FIGURE 29. Rectangular face graph representations for H_{12}, H_{13}, H_{14}.

The next cases are for torus with hole graphs with

$$|V(\partial G)| = 5, \quad |E(\partial G)| = 8.$$

Here the detachment map covers one edge of the boundary graph twice and two further vertices, v, w are covered twice. Such a graph in $\mathcal{T}$ is the graph H_{15} in Figure 30. This has cyclic type $v1e1w2v1e1w1$ and we note that the v and w vertices are alternating. The only other possible cyclic type is the nonalternating case $v1e1v2w1e1w1$. Arguing as in the previous nonalternating case (depicted in Figure 25) it follows that the graph G cannot be $(3,6)$-tight.
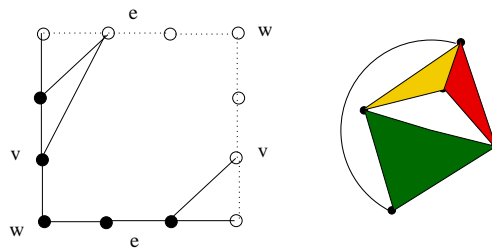

FIGURE 30. The graph H_{15} and its facial structure.

We next consider the case

$$|V(\partial G)| = 5, \quad |E(\partial G)| = 7.$$

Note that up to relabelling and order there is one form of cyclic word, namely $e1f2e1f1$, and so one form of detachment map for graphs in $\mathcal{T}$. Figure 31 indicates a vertex minimal representative, H_{16}, for this type.
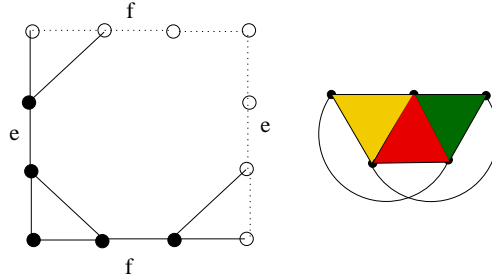

FIGURE 31. The graph H_{16} with detachment map type $e1f2e1f1$.

Finally we consider the case of boundary graphs with 4 vertices. There is one possible form of detachment map, with cyclic word $ef1ge1fg1$. A vertex minimal representative is given by the graph H_{17} in $\mathcal{T}$ in Figure 32.
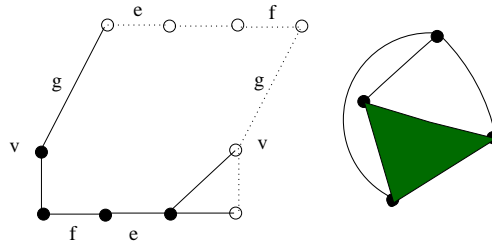

FIGURE 32. The graph H_{17} with detachment type $ef1ge1fg1$.

Note that K_3 is not a torus with hole graph G arising from any triple (T, D, i) where D is a 9-cycle. To see this note that the map $i : \partial D \to \partial G$ must cover at least one edge of ∂G more than twice. On the other hand each edge of G is incident to at most 2 faces, and i is injective on faces, so this is not possible. $\qquad\square$

7.1. **The uncontractible graphs in $\mathcal{T}$.** We next identify the graphs in $\mathcal{T}$ that are uncontractible.

Note first that H_{16} and H_{17} are uncontractible. Also it is straightforward to check, with the assistance of Lemmas 5.5 and 5.6, that the particular graphs $H_2, \ldots, H_{15}$ are contractible in $\mathcal{T}$, and indeed, are completely contractible to one of these two graphs.

However, it remains to check that every graph with no interior vertices is similarly con-tractible. To see this we argue in a case-by-case manner according to boundary type. The arguments become progressively simpler as the number of vertices decreases.

The $9v$ case, corresponding to the detachment map α_1 is covered by Lemma 5.7. (Al-ternatively one can effect a proof in the style of the following argument for the $v3v6$ case.)

7.2. The α_2, α_3 cases; types $v3v6$, $v4v5$, with $|V(G)| = 8$. Assume that $G \in \mathcal{T}$ is of type $v3v6$ and that G is uncontractible. We shall obtain a contradiction.

Since the boundary is of type $v3v6$ the vertex v is of degree 4 or more. Also there are no vertices of degree 3 incident to an FF edge, in view of Lemma 5.5.

We now consider the possibilities for an embedded graph representation of G which has been "standardised" so that

(i) the $v3v$ subcycle of the boundary cycle, with vertex sequence v, x, y, v, appears as the right hand boundary of a representing rectangle for $S^1 \times S^1$.

(ii) the first two edges, vw, wz of the $v6v$ subcycle appear on the lower boundary of the representing rectangle for $S^1 \times S^1$.

The embedded representation of G may be partially indicated, as in Figure 33. The upper boundary of the diagram is represented by the embeddings of the edges vw, wz and a path τ, which is not necessarily a path of embedded edges. The remaining embedded edges of G are representable by paths in the region R which may pass across τ a number of times. (That the degree of vertices is at least 4 is suggested by emerging edge paths.)
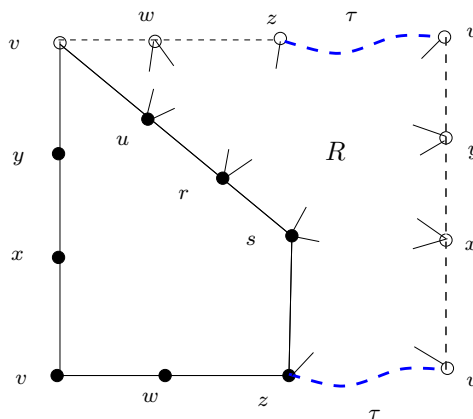

FIGURE 33. A partial embedded graph representation of a graph of type $v3v6$ with no interior vertices.

Suppose first that the crossover edge uw exists. It does not lie on a critical cycle, by Lemma 5.6 and so uw lies on a nonfacial 3-cycle (since otherwise G is contractible). From the standardised diagram it follows that this nonfacial 3-cycle has vertices u, w, z. We may assume that the embedded path in the diagram representing the edge wz is a path from w to z in R. This now implies that there is a hole separating cycle of length less than 9, a contradiction.

Since the edge uw does not exist the face incident to vu has edges va and ua with $a \neq w$, and va must be represented by an embedded curve in R starting from the upper left representative of v. If a is one of r, s or z then we obtain a contradiction as before. On the other hand since G is simple, without loop edges or multiple edges between the same vertices, the vertex a cannot be equal to v, x or y, and so we have the desired contradiction.

There is similar argument for the case $v4v5$.

7.3. **The α_4 case; type $e3e4$ with $|V(G)| = 7$.** Let $G \in \mathcal{T}$ be a graph of this type and assume that G is not contractible. Once again we may partially represent G as an embedded graph on the torus as indicated in Figure 34. By Lemma 5.5 the degree of each of the vertices z, r, s, x, y is at least 4.

In particular there are pairs of edges from each vertex r, s, y, x which are of FF type and which (as before) must lie on nonfacial 3-cycles. Considering an FF edge out of y the only possibilities are (i) yw, or (ii) yz, which requires ys (for the nonfacial 3-cycle), or (iii) ys which requires either sv or yz. Since there are at least 2 edges out of y it follows that (ii) or case (iii) must hold. However, case (ii), with yz and ys, cannot hold for the following reason. The triangulation would require the edge ry and this edge would not lie on a nonfacial 3-cycle (in any triangulation). Similarly, the remaining case (iii), with edges sy and sv, would require the edge sx and in any completing triangulation this would not lie on a nonfacial 3-cycle. Thus we obtain a contradiction in all cases.
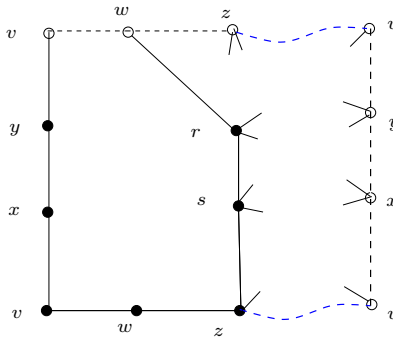

FIGURE 34. An embedded graph partial representation of G.

7.4. **The cases $\alpha_5, \ldots, \alpha_9$.** Suppose, by way of contradiction that there exists an uncontractible graph $G \in \mathcal{T}$ where the detachment map has one of these forms, so that there are no repeated edges and exactly two repeated vertices. Since every edge of ∂G lies on a face it follows from Lemma 5.5, that we may assume that each vertex is of degree at least 4. Since there are 7 vertices it follows that there are at least 7 crossover edges. This is a contradiction since there are 9 noncrossover edges and by $(3, 6)$-tightness there are 15 edges in total.

7.5. **The cases $\alpha_{10}, \ldots, \alpha_{15}$.** Consider a graph $G \in \mathcal{T}$ with no interior vertices and detachment map α_{10}. In an embedded graph representation on the torus we can assume that (in the edge identified rectangular representation) the repeated vertex x appears in the

corners and the repeated vertices v and w appear on opposite sides. Thus we have the representation in Figure 35. In this case note that we can assume that the boundary of the rectangle is provided by the edges of the 9-cycle for the hole together with some edge repetitions.
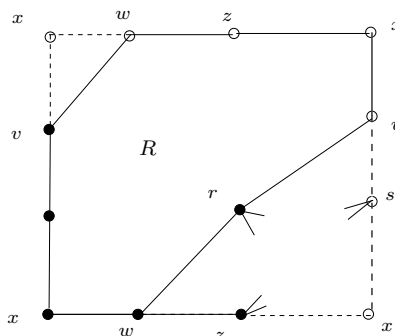

FIGURE 35. An embedded graph partial representation for the α_{10} case $v1w2x1v2w1x2$.

As before if we assume that G is uncontractible then the degrees of the vertices r, s and z are at least 4. By $(3, 6)$-tightness there are 3 crossover edges. It follows that the degrees are exactly 4. We thus see that there is only one triangulation and so G is equal to H_{10} which is contractible, a contradiction.

The cases $\alpha_{11}, \ldots, \alpha_{15}$ are similarly straightforward, with a unique triangulation.

References

[1] A. Cauchy, Sur les polygones et polyèdres. Second Mémoir. J École Polytechn. 9 (1813) 87-99; Oeuvres. T. 1. Paris 1905, pp. 26-38.

[2] R. Connelly, P.W. Fowler, S.D. Guest, B. Schulze, and W. Whiteley, When is a symmetric pin-jointed framework isostatic?, International Journal of Solids and Structures, 46 (2009), 762-773.

[3] J. Cruickshank, D. Kitson and S.C. Power, The generic rigidity of triangulated spheres with blocks and holes, Journal of Combinatorial Theory, Series B. 122 (2017), 550-577.

[4] M. Dehn, Über die starreit konvexer polyeder, Math. Ann. 77 (1916), 466-473.

[5] A.L. Fogelsanger, The generic rigidity of minimal cycles, PhD Thesis, Department of Mathematics, University of Cornell, 1988.

[6] J. Graver, B. Servatius and H. Servatius, Combinatorial rigidity. Graduate Studies in Mathematics, 2. American Mathematical Society, Providence, RI, 1993.

[7] H. Gluck, Almost all simply connected closed surfaces are rigid, in Geometric Topology, Lecture Notes in Math., no. 438, Springer-Verlag, Berlin, 1975, pp. 225-239.

[8] S. Lavrenchenko, Irreducible triangulations of a torus, Ukrain. Geom. Sb., 30 (1987), 52-62; translation in: J. Soviet Math., 51 (5) (1990), pp. 2537-2543.

[9] B. Schulze and S. Tanigawa, Infinitesimal rigidity of symmetric bar-joint frameworks, SIAM Journal on Discrete Mathematics, 29 (2015), 1259-1286.

[10] W. Whiteley, Vertex splitting in isostatic frameworks, Structural Topology, 16 (1990), 23-30.

DEPT. MATH. STATS., LANCASTER UNIVERSITY, LANCASTER LA1 4YF, U.K.
E-mail address: s.power@lancaster.ac.uk
E-mail address: james.cruickshank@nuigalway.ie
E-mail address: d.kitson@lancaster.ac.uk